A STUDY OF FATIGUE AND FRACTURE IN 7075-T6 ALUMINUM ALLOY IN VACUUM AND AIR ENVIRONMENTS

by C. Michael Hudson

Langley Research Center
Hampton, Va. 23665

1. Report No. NASA TN D-7262	2. Government Accession No.	3. Recipient's Catalog No.
4. Title and Subtitle A STUDY OF FATIGUE AND FRACTURE IN 7075-T6 ALUMINUM ALLOY IN VACUUM AND AIR ENVIRONMENTS		5. Report Date October 1973
		6. Performing Organization Code
7. Author(s) C. Michael Hudson		8. Performing Organization Report No. L-8829
9. Performing Organization Name and Address NASA Langley Research Center Hampton, Va. 23665		10. Work Unit No. 501-22-02-01
		11. Contract or Grant No.
12. Sponsoring Agency Name and Address National Aeronautics and Space Administration Washington, D.C. 20546		13. Type of Report and Period Covered Technical Note
		14. Sponsoring Agency Code

15. Supplementary Notes

Some of the information presented herein was included in a thesis entitled "An Experimental Investigation of the Effects of Vacuum Environment on the Fatigue Life, Fatigue-Crack-Growth Behavior, and Fracture Toughness of 7075-T6 Aluminum Alloy," offered in partial fulfillment of the requirements for the degree of Doctor of Philosophy in Materials Engineering, North Carolina State University, Raleigh, North Carolina, 1972.

16. Abstract

Axial-load fatigue-life, fatigue-crack-propagation, and fracture-toughness experiments were conducted on sheet specimens made of 7075-T6 aluminum alloy. These experiments were conducted at pressures ranging from atmospheric to 7 μPa (5×10^{-8} torr) to determine the effect of air pressure on fatigue behavior.

Analysis of the results from the fatigue-life experiments indicated that for a given stress level, lower air pressures produced longer fatigue lives. At a pressure of 7 μPa (5×10^{-8} torr) fatigue lives were 15 or more times as long as at atmospheric pressure.

Analysis of the results from the fatigue-crack-propagation experiments indicated that for small stress-intensity-factor ranges the fatigue-crack-propagation rates were up to twice as high at atmospheric pressure as in vacuum. An empirical equation developed by Forman, Kearney, and Engle (Trans. ASME, Ser. D.: J. Basic Eng., Sept. 1967) fit these rate data quite well.

The fracture toughness of 7075-T6 was unaffected by the vacuum environment.

Fractographic examination showed that specimens tested in both vacuum and air developed fatigue striations. Considerably more striations developed on specimens tested at atmospheric pressure, however.

17. Key Words (Suggested by Author(s)) Environmental effect Fatigue life Fatigue-crack propagation Fracture toughness 7075-T6 aluminum alloy	18. Distribution Statement Unclassified — Unlimited	
19. Security Classif. (of this report) Unclassified	20. Security Classif. (of this page) Unclassified	21. No. of Pages 36
		22. Price* Domestic, $3.00 Foreign, $5.50

A STUDY OF FATIGUE AND FRACTURE IN 7075-T6 ALUMINUM ALLOY IN VACUUM AND AIR ENVIRONMENTS*

By C. Michael Hudson
Langley Research Center

SUMMARY

Axial-load fatigue-life, fatigue-crack-propagation, and fracture-toughness experiments were conducted on sheet specimens made of 7075-T6 aluminum alloy. These experiments were conducted at pressures ranging from atmospheric to 7 μPa $(5 \times 10^{-8}$ torr) to determine the effect of air pressure on fatigue behavior.

Analysis of the results from the fatigue-life experiments indicated that for a given stress level, lower air pressures produced longer fatigue lives. At a pressure of 7 μPa $(5 \times 10^{-8}$ torr) fatigue lives were 15 or more times as long as at atmospheric pressure.

Analysis of the results from the fatigue-crack-propagation experiments indicated that for small stress-intensity-factor ranges the fatigue-crack-propagation rates were up to twice as high at atmospheric pressure as in vacuum. An empirical equation developed by Forman, Kearney, and Engle (Trans. ASME, Ser. D.: J. Basic Eng., Sept. 1967) fit these rate data quite well.

The fracture toughness of 7075-T6 was unaffected by the vacuum environment.

Fractographic examination showed that specimens tested in both vacuum and air developed fatigue striations. Considerably more striations developed on specimens tested at atmospheric pressure, however.

---

*Some of the information presented herein was included in a thesis entitled "An Experimental Investigation of the Effects of Vacuum Environment on the Fatigue Life, Fatigue-Crack-Growth Behavior, and Fracture Toughness of 7075-T6 Aluminum Alloy," offered in partial fulfillment of the requirements for the degree of Doctor of Philosophy in Materials Engineering, North Carolina State University, Raleigh, North Carolina, 1972.

INTRODUCTION

Engine and thruster firings, thermal cycles, and other kinetic loading sources can produce fatigue loadings on spacecraft structures in low-pressure environments. Although some fatigue tests have been made on pure metals in a vacuum (ref. 1), relatively little is known about the vacuum-fatigue behavior of most structural alloys. Consequently, in the present study a series of fatigue-life, fatigue-crack-propagation, and fracture-toughness specimens of 7075-T6 aluminum alloy were tested at various air pressures to demonstrate the effects of environment on the three phases of the fatigue phenomenon. These data will also provide baseline information for future investigations into the effects of different gas environments on the fatigue behavior of 7075-T6.

Three ultrahigh-vacuum chambers containing fatigue-loading frames were used for the experiments. The fatigue-life specimens were tested at various pressures from atmospheric to 7 μPa (5×10^{-8} torr). The fatigue-crack-propagation and fracture-toughness specimens were tested at two pressures: atmospheric and 7 μPa (5×10^{-8} torr).

The fatigue-crack-propagation and fracture-toughness data were correlated with stress-intensity parameters. Such correlations are useful for predicting crack propagation in complex structures. For example, Poe (ref. 2) showed that fatigue-crack growth in stiffened panels can be predicted from stress-intensity parameters plus the data from tests of simple sheet specimens. An empirical equation developed by Forman, Kearney, and Engle (ref. 3) was fitted by the least-squares technique to the fatigue-crack propagation data. The fracture surfaces of selected specimens were examined with transmission and scanning electron microscopes to study fracture modes in vacuum and in air.

SYMBOLS

The physical quantities in this paper are given both in the International System of Units (SI) and in U. S. Customary Units. The measurements and calculations were made in U. S. Customary Units. Factors relating the two systems are given in reference 4 and those used in the present investigation are presented in appendix A.

a one-half of total length of a central crack, mm (in.)

a_c one-half of total crack length at the onset of unstable crack growth, mm (in.)

C constant in fatigue-crack-propagation equation

da/dN rate of fatigue-crack propagation, nm/cycle (in./cycle)

E Young's modulus of elasticity, GN/m^2 (psi)

e elongation in gage length of 51 mm (2 in.), percent

K_c critical stress-intensity factor at failure, $MN/m^{3/2}$ (psi-in$^{1/2}$)

K_{max} maximum stress-intensity factor, $MN/m^{3/2}$ (psi-in$^{1/2}$)

K_{min} minimum stress-intensity factor, $MN/m^{3/2}$ (psi-in$^{1/2}$)

K_T theoretical elastic stress-concentration factor

ΔK stress-intensity-factor range, $MN/m^{3/2}$ (psi-in$^{1/2}$)

LN_2 liquid nitrogen

N number of cycles

n exponent in fatigue-crack-propagation equation

P_a amplitude of load applied in a cycle, N (lbf)

P_c load on specimen immediately prior to rapid fracture, N (lbf)

P_m mean load applied in a cycle, N (lbf)

P_{max} maximum load applied in a cycle, $P_m + P_a$, N (lbf)

P_{min} minimum load applied in a cycle, $P_m - P_a$, N (lbf)

R ratio of minimum stress to maximum stress

S_{max} gross maximum stress, P_{max}/wt, MN/m^2 (psi)

S'_{max} net maximum stress, $P_{max}/(w - x)t$, MN/m^2 (psi)

S_{min} gross minimum stress, P_{min}/wt, MN/m^2 (psi)

t   specimen thickness, mm (in.)

w   specimen width, mm (in.)

x   width of a central notch, mm (in.)

α secant correction factor for finite width of panel

σ_u ultimate tensile strength, MN/m^2 (psi)

σ_y yield strength (0.2-percent offset), MN/m^2 (psi)

EXPERIMENTAL PROCEDURES

Specimens

General. - All fatigue-life, fatigue-crack-propagation, and fracture-toughness specimens were made from a special stock of 7075-T6 aluminum alloy, 2.3 mm (0.090 in.) thick, retained at Langley Research Center for fatigue testing. (Tensile properties are listed in table I.) The longitudinal axis of all specimens was parallel to the rolling direction of the sheet material.

Fatigue-life specimens. - Figure 1 shows the configurations of the fatigue-life specimens. Scratches and tool marks on the unnotched specimens were removed by fine hand polishing. This polishing was done in the longitudinal direction of the specimen to preclude transverse polishing marks. After polishing, the average surface roughness of the unnotched specimens was about 150 nm rms (6 μin. rms).

Surface scratches on the notched specimens were removed by moderate hand polishing. The notch was cut into the center of the specimens by first drilling two holes 2.95 mm (0.116 in.) in diameter on either side of the center line and then drilling a hole

4

6.35 mm (0.250 in.) in diameter in the center of the specimen. The resulting notch configuration approximates an ellipse having a stress-concentration factor of 4.1 (ref. 5). A rotating rubber rod impregnated with an abrasive was used to deburr the perimeter of the notch. This deburring procedure produced a slight bevel around the circumference of the notch.

Fatigue-crack-propagation and fracture-toughness specimens. - Figure 2 shows the configuration of the fatigue-crack-propagation and fracture-toughness specimens. A notch 2.54 mm (0.10 in.) long by 0.25 mm (0.01 in.) wide was cut into the center of each specimen by an electrical-discharge machining process. The heat-affected zone resulting from this process is less than 0.25 mm (0.01 in.) wide. Consequently, after crack initiation, all of the material through which the fatigue crack propagated was unaltered by the cutting process.

One side of each specimen bore a reference grid (ref. 6) for crack-propagation tracking. No detrimental effects of the grid were observed in metallographic examinations and tensile tests of specimens bearing the grid.

Testing Equipment

Vacuum-fatigue testing systems. - Experiments were conducted in three vacuum-fatigue testing systems. (See appendix B.) Basically, each system consisted of an ultra-high-vacuum chamber mounted on an axial-load fatigue testing machine. The vacuum chamber enclosed the machine's specimen-mounting apparatus, which included the specimen grips and the upper portions of the loading ram and load-reaction frame. Each fatigue machine had a load capacity of ±89 kN (±20 000 lbf). Two of the fatigue machines were driven by closed-loop hydraulic-loading units at frequencies between 13 and 23 Hz (780 and 1380 cpm). The third was mechanically driven at a subresonant frequency of 30 Hz (1800 cpm). Loads were continuously monitored on these machines by measuring the output of a dynamometer in series with the specimens. The maximum error in loading was less than ±1 percent of the required maximum load.

The vacuum-chamber section of each system was a vertical stainless-steel cylinder · that had a horizontal parting plane in the middle for access. A mechanical pump maintained a medium vacuum, and a diffusion pump maintained a high vacuum. Water-cooled and liquid-nitrogen-cooled baffles trapped oil vapors streaming back from the diffusion pump. The vacuum chambers contained cryopanels which were cooled with liquid nitrogen

to accelerate pumping for tests at 7 μPa (5×10^{-8} torr). However, these cryopanels tended to cool the specimens; consequently, quartz-tube lamps were used to maintain the specimens at room temperature. For tests at higher pressures, the cryopanels, and consequently the lamps, were not required.

Ancillary tests showed that the specimen temperature could be satisfactorily regulated by controlling the temperature of a tab mounted next to the specimen. A temperature-control unit, supplied with the signal from a thermocouple on the tab, maintained room temperature.

A pressure-control unit automatically maintained the desired air pressure inside the chamber by admitting quantities of dry air. Thermocouple gages measured chamber pressures between 133 Pa and 133 mPa (1 torr and 1×10^{-3} torr); ionization gages measured pressures between 133 mPa and 7 μPa (1×10^{-3} and 5×10^{-8} torr).

Detailed descriptions of similar hydraulic and subresonant loading systems are given in references 7 and 8, respectively. Detailed descriptions of the vacuum and temperature-control systems are given in appendix B of this report.

Electron microscopes. - Transmission and scanning electron microscopes were used to study the fatigue-fracture surfaces of selected specimens. Two-stage carbon-platinum replicas of the fracture surfaces were studied in the transmission electron microscope. The fracture surfaces were studied directly in the scanning electron microscope.

Test Procedure

General. - Axial-load fatigue-life, fatigue-crack-propagation, and fracture-toughness experiments were conducted. Experiments at atmospheric pressure were conducted in laboratory air. Experiments at lower pressures were conducted in dry air which was admitted to the chamber by the automatic pressure controller.

In all fatigue-life and fatigue-crack-propagation experiments, a stress ratio R of 0.02 was used, and the mean and alternating loads were constant throughout each test.

Fatigue-life experiments. - Most of the unnotched and all of the notched fatigue-life specimens were tested at either atmospheric pressure or 7 μPa (5×10^{-8} torr). Additional unnotched specimens were tested at pressures of 67 Pa, 7 Pa, and 67 mPa

$(5 \times 10^{-1}, 5 \times 10^{-2},$ and 5×10^{-4} torr) to establish the variation of fatigue life with decreasing pressure.

Fatigue-crack-propagation experiments. - The center-notched fatigue-crack-propagation specimens were tested at atmospheric pressure and 7 μPa $(5 \times 10^{-8}$ torr) Fatigue-crack propagation was visually observed through ports in the chamber wall. The number of cycles required to propagate the crack to each grid line was recorded so that crack-propagation rates could be determined. All tests were terminated when the fatigue cracks reached predetermined crack lengths; these specimens were then tested for fracture toughness.

Fracture-toughness experiments. - The unfailed crack-propagation specimens were immediately loaded to failure in situ at the same air pressures that were used in the crack-propagation experiments. During the fracture tests, the load-cell output was recorded on an oscillograph in order to determine the load at failure. The photographic grid provided a visual reference of the crack tip location at the onset of the unstable crack growth which occurred at P_c. The loading rate in these fracture-toughness experiments was approximately 1500 N/s (20 000 lbf/min).

RESULTS

The special stock of 7075-T6 aluminum alloy used in this investigation is more than 20 years old. Consequently, a preliminary study was conducted to determine whether the fatigue properties of the 7075-T6 had changed in 20 years. In this preliminary study, the data scatter band from fatigue-life tests conducted about 20 years ago on specimens made from this stock (ref. 8) was compared with data from similar tests conducted as part of this investigation (fig. 3). The close agreement between the data from this investigation and the data scatter band from reference 8 indicates that the fatigue resistance of the 7075-T6 has changed very little over the 20-year period.

Fatigue-Life Experiments

Tables II and III present the results of the fatigue-life experiments on the unnotched and notched specimens, respectively. These tables give the maximum stress and fatigue life for each specimen at the various air pressures of the tests.

Figure 4 shows the variation of fatigue life with gross maximum stress for the unnotched specimens at various air pressures. A curve is faired through each set of data. Symbols with arrows represent tests in which the specimens did not fail in 5 000 000 or more cycles. Numbers under some symbols indicate the number of specimens having essentially the same fatigue life.

Figure 5, which shows the curves from figure 4 on a single plot, indicates that for a given stress level, lower air pressures produced longer fatigue lives. For S_{max} between 410 and 290 MN/m^2 (60 and 42×10^3 psi), fatigue lives were 15 to 100 times longer at an air pressure of 7 μPa (5×10^{-8} torr) than at atmospheric pressure, 101 kPa (760 torr). The fatigue limit (taken at 5×10^6 cycles) was about 70 MN/m^2 (10×10^3 psi) higher at an air pressure of 7 μPa (5×10^{-8} torr) than at atmospheric pressure.

It should be noted that the variation of fatigue life with gas pressure has not been established to date for all aluminum alloys. In some instances, a continuous increase in fatigue life with decreasing gas pressure was found (as in the investigation reported herein), whereas in other instances, a stepwise increase occurred at some critical pressure level (ref. 1).

Figure 6 shows the variation of fatigue life with net maximum stress for the notched (K_T = 4.1) specimens. For S'_{max} between 207 and 117 MN/m^2 (30 and 17×10^3 psi), fatigue lives were 5 to 15 times longer at an air pressure of 7 μPa (5×10^{-8} torr) than at atmospheric pressure. In contrast to the results for the unnotched specimens, the fatigue limit was only slightly higher at 7 μPa (5×10^{-8} torr) than at atmospheric pressure.

Several investigators (refs. 9 and 10) have suggested that specimens having $K_T \approx 4$ notches exhibit fatigue behavior like that of contemporary aerospace structures. If so, the results for the K_T = 4.1 specimens, as well as those for the unnotched specimens discussed earlier, indicate that the space environment may significantly increase the fatigue resistance of space-vehicle structures provided, of course, that other space phenomena such as micrometeorite impingement and heavy radiation fluxes do not have overriding deleterious effects.

A literature review included in reference 11 indicates that the most probable cause of the increased fatigue life at reduced air pressures observed in this investigation is the exclusion of water vapor from the environment surrounding the test specimens.

Fatigue-Crack-Propagation Experiments

Table IV presents the results of the fatigue-crack-propagation experiments. These data were used to plot crack half-length against cycles, curves were faired through the data points, and then fatigue-crack-propagation rates da/dN were obtained by constructing tangents to the curves. These rates are plotted against the stress-intensity-factor range ΔK in figure 7. (Appendix C describes the use of ΔK in correlating fatigue-crack-propagation data.) At both atmospheric pressure and 7 μPa (5×10^{-8} torr), fatigue-crack-propagation rates were single-valued functions of ΔK. For the lower values of ΔK, the fatigue-crack-propagation rates under vacuum were approximately one-half those at atmospheric pressure. However, for the higher values of ΔK, the crack-propagation rates were about the same in vacuum and at atmospheric pressure.

An empirical fatigue-crack-propagation equation developed by Forman, Kearney, and Engle (ref. 3) fits the data of figure 7 quite well. This equation has the form:

$$\frac{da}{dN} = \frac{C(\Delta K)^n}{(1 - R)K_c - \Delta K} \tag{1}$$

The values of K_c were determined in the fracture-toughness portion of this investigation. The values of C and n were determined by using the least-squares technique and are listed in the following table:

Pressure	C	n	Units for —		
			da/dN	ΔK	K_c
SI system					
Atmospheric (101 kPa)	23.57	2.44	nm/cycle	$MN/m^{3/2}$	$MN/m^{3/2}$
7 μPa	2.81	3.02			
U.S. system					
Atmospheric (760 torr)	5.19×10^{-11}	2.44	in./cycle	$psi\text{-}in^{1/2}$	$psi\text{-}in^{1/2}$
5×10^{-8} torr	1.19×10^{-13}	3.02			

Fracture Toughness Experiments

Table V presents the results of the fracture-toughness experiments. This table gives a_c (the half-length of the crack at the onset of unstable crack growth), P_c (the load on the specimen immediately preceding rapid fracture), and K_c (the critical stress-intensity factor at failure). Figure 8 shows the variation of K_c with a_c for tests at both atmospheric pressure and 7 μPa (5×10^{-8} torr). Generally, K_c was constant for all values of a_c. Moreover, the average value of K_c for tests conducted at both pressures was the same, indicating that the environment had no effect on fracture toughness.

Fractographic Examination

Fractographs of unnotched specimens were made with both transmission and scanning electron microscopes. Figure 9 shows fractographs of specimens tested at atmospheric pressure. Fatigue striations are clearly visible in these photographs. At the lower stress levels, numerous large patches of these striations appeared on the fracture surface. At higher stress levels, smaller, moderately spaced patches of striations appeared. At all stress levels, these patches were readily discernible.

Figure 10 shows fractographs of specimens tested at 7 μPa (5×10^{-8} torr). A thorough search of the specimen's fracture surfaces with the scanning electron microscope revealed small, very widely scattered patches of fatigue striations. However, the transmission electron microscope revealed no such striations. The striations which formed in vacuum either did not replicate well or were frequently obscured by the copper grid that holds the replicas in the transmission electron microscope.

DISCUSSION

The fatigue phenomenon is generally considered to consist of three phases: crack initiation, crack propagation, and fracture. In this investigation the effects of vacuum environment on each of these phases were studied. The effects on the crack-propagation and fracture phases were studied directly; the effects on the crack-initiation phase were deduced from the results of the fatigue-life experiments, which included all three phases. These studies showed that for 7075-T6 aluminum alloy (a) the fatigue lives of unnotched specimens could be 15 or more times longer in vacuum than at atmospheric pressure; (b) fatigue-crack-propagation rates were lower by, at most, a factor of 2 in vacuum than

at atmospheric pressure; and (c) the fracture toughness in vacuum and at atmospheric pressure was the same. Consideration of these findings indicates that crack initiation was the phase most significantly affected by vacuum. In tests on pure aluminum and on aluminum alloys, Broom and Nicholson (ref. 12) and Ham and Reichenbach (ref. 13) also found that a vacuum environment significantly retarded the initiation of fatigue cracks. On the other hand, Bradshaw and Wheeler (ref. 14) and Wadsworth (ref. 15) found that fatigue cracks initiated in the same number of cycles in vacuum and at atmospheric pressure. The reason for this difference in findings is not apparent.

SUMMARY OF RESULTS

A series of fatigue-life, fatigue-crack-propagation, and fracture-toughness specimens were tested at various air pressures to study the effect of vacuum environment on fatigue behavior. These specimens were made of 7075-T6 aluminum alloy 2.3 mm (0.090 in.) thick. The results can be summarized as follows:

1. Crack initiation was the phase most affected by vacuum environment.

2. For a given stress level, lower air pressures produced longer fatigue lives.

3. Fatigue limits were higher in vacuum than at atmospheric pressure.

4. For small stress-intensity-factor ranges, the fatigue-crack-propagation rates in vacuum were approximately 50 percent of those at atmospheric pressure. For large stress-intensity-factor ranges, the fatigue-crack-propagation rates were about the same in vacuum as at atmospheric pressure.

5. The vacuum environment had no effect on the fracture toughness of 7075-T6 aluminum alloy.

6. Fatigue striations were found on the fracture surfaces of both air- and vacuum-tested specimens, but considerably more striations were found on the surfaces of the air-tested specimens.

Langley Research Center,
    National Aeronautics and Space Administration,
        Hampton, Va., July 12, 1973.

APPENDIX A

CONVERSION OF SI UNITS TO U.S. CUSTOMARY UNITS

The International System of Units (SI) was adopted by the Eleventh General Conference on Weights and Measures held in Paris in 1960 (ref. 4). Conversion factors required for units used herein are given in the following table:

Physical quantity	SI Unit (a)	Conversion factor (b)	U.S. Customary Unit
Force	newton (N)	0.2248	lbf
Length	meter (m)	0.3937×10^2	in.
Pressure	pascal (Pa)	0.7500×10^{-2}	torr
Stress	newtons per meter^2 (N/m^2)	0.145×10^{-3}	psi
Stress intensity	newtons per meter$^{3/2}$ (N/m$^{3/2}$)	0.9099×10^{-3}	psi-in$^{1/2}$
Frequency	hertz (Hz)	60	cpm

[a] Prefixes and symbols to indicate multiples of units are as follows:

Multiple	Prefix	Symbol
10^{-9}	nano	n
10^{-6}	micro	μ
10^{-3}	milli	m
10^3	kilo	k
10^6	mega	M
10^9	giga	G

[b] Multiply value given in SI Unit by conversion factor to obtain equivalent in U.S. Customary Unit.

APPENDIX B

VACUUM AND TEMPERATURE CONTROL SYSTEMS

Figure 11 is a schematic diagram of the vacuum pumping system. The minimum gas pressure for this system is 107 nPa (8×10^{-10} torr). A 254-mm (10-in.) diameter diffusion pump evacuated the chamber for tests in the high-vacuum range. A water-cooled baffle mounted above the diffusion pump inhibited back-streaming of pump-oil vapors. A liquid-nitrogen-cooled baffle mounted above the water-cooled baffle further inhibited back-streaming.

Either a mechanical roughing pump (which was also used to evacuate the chamber down to 6.7 Pa (5×10^{-2} torr)) or a mechanical holding pump maintained a pressure of 1.3 Pa (10^{-2} torr) at the exhaust of the diffusion pump.

An automatic pressure controller regulated the pressure inside the chamber. This controller actuated a variable-leak valve which admitted dry air into the chamber. The chamber pressure was controllable within the range from 133 Pa to 107 nPa (1 torr to 8×10^{-10} torr).

Thermocouple and ionization gages measured gas pressures inside the chamber. The thermocouple gage can measure pressures between 133 Pa and 133 mPa (1 torr and 1×10^{-3} torr). The ionization gage can measure pressures between 133 mPa and 107 nPa (1×10^{-3} and 8×10^{-10} torr).

The specimen-viewing ports were located 180° apart on the upper half of the chamber. Concentric pairs of O-rings sealed these ports, and another pair sealed the main flange of the vacuum system. A guard pump evacuated the area between these O-rings in order to reduce the pressure differential, and consequently the leakage, across the inner O-ring.

Feed-throughs carried electrical power, liquid nitrogen, and the signals from thermocouples through the chamber wall, and exposed the sensing elements of the ionization and thermocouple gages to the vacuum environment. Copper gaskets sealed these feed-throughs and the connection for the variable-leak valve.

Figure 12 is a schematic diagram of the specimen temperature-control system, which could control the specimen temperature within the range from 200 to 366 K (-100° to 200° F). The four banks of quartz-tube lamps, two on each side of the specimen, had

13

polished parabolic reflectors to concentrate the energy on the specimen. Separate temperature controllers regulated the lamps on each side of the specimen by using the thermocouple signal from a tab mounted next to the specimen.

Two oxygen-free high-conductivity copper cryopanels filled with liquid nitrogen cooled the specimen. Black paint with a minimum emittance of 0.9 made the inward-facing side of the cryopanels highly absorptive for rapid cooling of the specimen. Chrome plating made the outward-facing side of the cryopanel highly reflective (so that extraneous heat energy was not absorbed).

In addition to cooling the test specimen, the cryopanels helped to pump the system by condensing gases on the cryopanel surfaces. The cryopanels retained these gases until the fatigue experiment was completed. Level controllers automatically kept the cryopanels filled with liquid nitrogen during testing.

APPENDIX C

FATIGUE-CRACK-PROPAGATION ANALYSIS

The fatigue-crack-propagation data were correlated by the stress-intensity method. Paris (ref. 16) hypothesized that the rate of fatigue-crack propagation was a function of the stress-intensity range; that is,

$$\frac{da}{dN} = f(\Delta K) \tag{C1}$$

where

$$\Delta K = K_{max} - K_{min} \tag{C2}$$

For centrally cracked specimens subjected to a uniformly distributed axial load,

$$K_{max} = \alpha S_{max} \sqrt{a\pi} \tag{C3}$$

and

$$K_{min} = \alpha S_{min} \sqrt{a\pi} \tag{C4}$$

The term α is a factor intended to correct for the finite width of the specimen (ref. 17) and is given by

$$\alpha = \sqrt{\sec \frac{\pi a}{w}} \tag{C5}$$

REFERENCES

1. Hudson, C. Michael: Problems of Fatigue of Metals in a Vacuum Environment. NASA TN D-2563, 1965.

2. Poe, C. C., Jr.: Fatigue Crack Propagation in Stiffened Panels. Damage Tolerance in Aircraft Structures, Spec. Tech. Publ. No. 486, Amer. Soc. Testing Mater., 1971, pp. 79-97.

3. Forman, R. G.; Kearney, V. E.; and Engle, R. M.: Numerical Analysis of Crack Propagation in Cyclic-Loaded Structures. Trans. ASME, Ser. D.: J. Basic Eng., vol. 89, no. 3, Sept. 1967, pp. 459-464.

4. Anon.: Metric Practice Guide. E 380-72, Amer. Soc. Testing Mater., June 1972.

5. Imig, L. A.: Fatigue of SST Materials Using Simulated Flight-by-Flight Loading. Fatigue at Elevated Temperatures, Spec. Tech. Publ. No. 520, Amer. Soc. Testing Mater., 1973.

6. Hudson, C. Michael: Fatigue-Crack Propagation in Several Titanium and Stainless-Steel Alloys and One Superalloy. NASA TN D-2331, 1964.

7. Imig, L. A.: Effect of Initial Loads and of Moderately Elevated Temperature on the Room-Temperature Fatigue Life of Ti-8Al-1Mo-1V Titanium-Alloy Sheet. NASA TN D-4061, 1967.

8. Grover, H. J.; Hyler, W. S.; Kuhn, Paul; Landers, Charles B.; and Howell, F. M.: Axial-Load Fatigue Properties of 24S-T and 75S-T Aluminum Alloy as Determined in Several Laboratories. NACA Rep. 1190, 1954. (Supersedes NACA TN 2928.)

9. Spaulding, E. H.: Design for Fatigue. SAE Trans., vol. 62, 1954, pp. 104-116.

10. Naumann, Eugene C.; and Schott, Russell L.: Axial-Load Fatigue Tests Using Loading Schedules Based on Maneuver-Load Statistics. NASA TN D-1253, 1962.

11. Hudson, Charles Michael: An Experimental Investigation of the Effects of Vacuum Environment on the Fatigue Life, Fatigue-Crack-Growth Behavior, and Fracture Toughness of 7075-T6 Aluminum Alloy. Ph. D. Thesis, North Carolina State Univ., 1972.

12. Broom, Trevor; and Nicholson, Anthony: Atmospheric Corrosion-Fatigue of Age-Hardened Aluminum Alloys. J. Inst. Metals, vol. 89, Feb. 1961, pp. 183-190.

13. Ham, John L.; and Reichenbach, George S.: Fatigue Testing of Aluminum in Vacuum. Symposium on Materials for Aircraft, Missiles, and Space Vehicles, Spec. Tech. Publ. No. 345, Am. Soc. Testing Mater., c.1963, pp. 3-13.

14. Bradshaw, F. J.; and Wheeler, C.: The Effect of Environment on Fatigue Crack Propagation – 1. Measurements on Al. Alloy DTD 5070A, S.A.P., Pure Aluminium and a Pure Al-Cu-Mg Alloy. Tech. Rep. No. 65073, Brit. R.A.E., Apr. 1965.

15. Wadsworth, N. J.: The Effect of Environment on Metal Fatigue. Internal Stresses and Fatigue in Metals, Gerald M. Rassweiler and William L. Grube, eds., Elsevier Pub. Co. (Amsterdam), 1959, pp. 382-396.

16. Paris, Paul C.: The Fracture Mechanics Approach to Fatigue. Fatigue – An Interdisciplinary Approach, John J. Burke, Norman L. Reed, and Volker Weiss, eds., Syracuse Univ. Press, 1964, pp. 107-132.

17. Brown, William F.; and Srawley, John E.: Plane Strain Crack Toughness Testing of High Strength Metallic Materials. Spec. Tech. Publ. No. 410, Amer. Soc. Testing Mater., c.1966.

TABLE I.- TENSILE PROPERTIES OF THE 7075-T6 ALUMINUM ALLOY

Year of data	σ_u		σ_y		E		e, percent	No. of tests
	MN/m^2	psi	MN/m^2	psi	GN/m^2	psi		
1968	574	83 200	523	75 900	69.6	10.1×10^6	12	20
1949 (ref. 8)	572	82 900	518	75 500	70.5	10.2×10^6	12	152

TABLE II.- RESULTS OF FATIGUE-LIFE EXPERIMENTS

ON UNNOTCHED SPECIMENS (R = 0.02)

(a) Air pressure, 101 kPa (760 torr)

Specimen number	S_{max}		Fatigue life, cycles	Remarks
	MN/m^2	psi		
B83N7-47	414	60 000	8 590	
B83N7-45	414	60 000	10 320	
B83N7-46	414	60 000	16 810	
B83N7-42	414	60 000	18 560	
B65N7-125	414	60 000	22 550	
B84N7-59	345	50 000	27 660	
B71N7-184	345	50 000	27 710	
B71N7-181	345	50 000	35 040	
B84N7-53	345	50 000	42 130	
B84N7-56	345	50 000	46 990	
B71N7-183	276	40 000	47 290	
B71N7-182	276	40 000	54 970	
B71N7-188	276	40 000	74 020	
B71N7-189	276	40 000	79 260	
B84N7-57	276	40 000	145 640	
B72N7-196	276	40 000	195 930	
B88N7-93	241	35 000	239 090	
B65N7-126	241	35 000	1 405 500	
B65N7-130	241	35 000	4 246 550	
B88N7-99	241	35 000	>5 113 230	Did not fail
B84N7-52	241	35 000	>5 376 110	Did not fail
B72N7-197	241	35 000	>6 135 730	Did not fail
B69N7-168	228	33 000	134 340	
B83N7-43	228	33 000	421 500	
B65N7-123	228	33 000	440 540	
B65N7-124	228	33 000	2 337 380	
B69N7-162	228	33 000	>5 000 000	Did not fail
B69N7-166	228	33 000	>5 009 850	Did not fail
B83N7-44	228	33 000	>5 012 250	Did not fail
B74N7-15	228	33 000	>9 066 790	Did not fail

TABLE II.- RESULTS OF FATIGUE-LIFE EXPERIMENTS

ON UNNOTCHED SPECIMENS (R = 0.02) — Continued

(b) Air pressure, 67 Pa $(5 \times 10^{-1}$ torr)

Specimen number	S_{max}		Fatigue life, cycles	Remarks
	MN/m^2	psi		
B64N7-120	414	60 000	78 220	
B88N7-92	414	60 000	94 580	
B64N7-111	414	60 000	116 360	
B83N7-49	345	50 000	101 020	
B69N7-161	345	50 000	101 070	
B65N7-129	345	50 000	140 340	
B74N7-17	310	45 000	221 740	
B56N7-5	310	45 000	844 830	
B60N7-7	310	45 000	1 159 740	
B64N7-114	276	40 000	1 264 000	
B87N7-90	276	40 000	>5 004 290	Did not fail
B87N7-86	276	40 000	>8 181 610	Did not fail

(c) Air pressure, 7 Pa $(5 \times 10^{-2}$ torr)

Specimen number	S_{max}		Fatigue life, cycles	Remarks
	MN/m^2	psi		
B68N7-157	414	60 000	89 600	
B86N7-80	414	60 000	140 450	
B74N7-18	414	60 000	146 370	
B69N7-165	345	50 000	83 190	
B69N7-170	345	50 000	98 880	
B69N7-167	345	50 000	114 210	
B69N7-169	345	50 000	124 790	
B65N7-128	345	50 000	171 840	
B83N7-50	345	50 000	225 090	
B74N7-16	310	45 000	711 870	
B87N7-83	310	45 000	1 047 810	
B63N7-103	310	45 000	1 168 970	
B68N7-158	276	40 000	>5 201 580	Did not fail
B86N7-74	276	40 000	>7 095 840	Did not fail

TABLE II.- RESULTS OF FATIGUE-LIFE EXPERIMENTS

ON UNNOTCHED SPECIMENS (R = 0.02) — Concluded

(d) Air pressure, 67 mPa $(5 \times 10^{-4}$ torr)

Specimen number	S_{max}		Fatigue life, cycles	Remarks
	MN/m^2	psi		
B74N7-14	414	60 000	180 310	
B87N7-81	414	60 000	188 740	
B49N7-7	414	60 000	379 170	
B52N7-1	345	50 000	251 960	
B74N7-19	345	50 000	359 780	
B74N7-12	345	50 000	517 600	
B87N7-84	310	45 000	340 400	
B58N7-3	310	45 000	375 000	
B52N7-9	310	45 000	>5 000 300	Did not fail
B58N7-1	310	45 000	5 197 200	
B86N7-71	276	40 000	2 442 500	
B68N7-156	276	40 000	>5 008 710	Did not fail
B87N7-87	276	40 000	>5 049 570	Did not fail
B64N7-118	276	40 000	>7 106 710	Did not fail

(e) Air pressure, 7 μPa $(5 \times 10^{-8}$ torr)

Specimen number	S_{max}		Fatigue life, cycles	Remarks
	MN/m^2	psi		
B64N7-117	414	60 000	137 790	
B88N7-98	414	60 000	155 460	
B86N7-77	414	60 000	296 560	
B72N7-192	414	60 000	364 880	
B72N7-194	414	60 000	570 870	
B64N7-119	345	50 000	583 300	
B68N7-153	345	50 000	634 310	
B72N7-191	345	50 000	874 000	
B64N7-115	345	50 000	954 680	
B88N7-100	345	50 000	1 194 830	
B63N7-104	345	50 000	1 319 420	
B86N7-75	345	50 000	1 412 010	
B64N7-112	310	45 000	625 200	
B74N7-11	310	45 000	805 020	
B63N7-107	310	45 000	1 956 270	
B86N7-79	310	45 000	2 119 710	
B64N7-113	310	45 000	2 496 230	
B87N7-88	276	40 000	>5 000 000	Did not fail
B87N7-82	276	40 000	>5 799 290	Did not fail
B87N7-85	276	40 000	>7 992 310	Did not fail
B63N7-105	276	40 000	>8 086 090	Did not fail
B63N7-106	276	40 000	>8 243 790	Did not fail

(a) Air pressure, 101 kPa (760 torr)

Specimen number	S'_{max}		Fatigue life, cycles	Remarks
	NM/m^2	psi		
B98N7-96	207	30 000	7 030	
B98N7-94	207	30 000	7 090	
B98N7-100	207	30 000	7 150	
B92N7-33	207	30 000	7 360	
B94N7-60	207	30 000	7 760	
B94N7-59	138	20 000	38 600	
B98N7-93	138	20 000	39 600	
B98N7-92	138	20 000	45 680	
B94N7-54	138	20 000	50 490	
B90N7-12	138	20 000	51 080	
B98N7-95	103	15 000	1 659 960	
B94N7-53	103	15 000	2 683 640	
B92N7-39	103	15 000	3 020 730	
B95N7-61	103	15 000	3 454 040	
B92N7-34	103	15 000	>5 033 660	Did not fail
B92N7-37	103	15 000	>5 394 790	Did not fail
B92N7-35	83	12 000	>5 000 310	Did not fail
B90N7-11	83	12 000	>5 000 330	Did not fail
B90N7-14	83	12 000	>5 086 160	Did not fail
B92N7-32	83	12 000	>5 261 970	Did not fail
B92N7-31	83	12 000	>5 277 000	Did not fail

(b) Air pressure, 7 μPa (5×10^{-8} torr)

Specimen number	S'_{max}		Fatigue life, cycles	Remarks
	MN/m^2	psi		
B94N7-51	207	30 000	27 410	
B95N7-64	207	30 000	29 600	
B95N7-69	207	30 000	40 060	
B92N7-38	207	30 000	42 090	
B95N7-68	207	30 000	59 240	
B90N7-19	138	20 000	323 580	
B92N7-40	138	20 000	611 130	
B90N7-20	138	20 000	688 730	
B94N7-52	138	20 000	724 900	
B92N7-36	138	20 000	802 960	
B95N7-63	124	18 000	502 980	
B95N7-66	124	18 000	580 490	
B95N7-62	124	18 000	1 150 820	
B95N7-70	124	18 000	1 268 800	
B95N7-65	124	18 000	1 956 620	
B91N7-24	103	15 000	1 444 350	
B91N7-30	103	15 000	2 895 970	
B95N7-67	103	15 000	>6 401 400	Did not fail

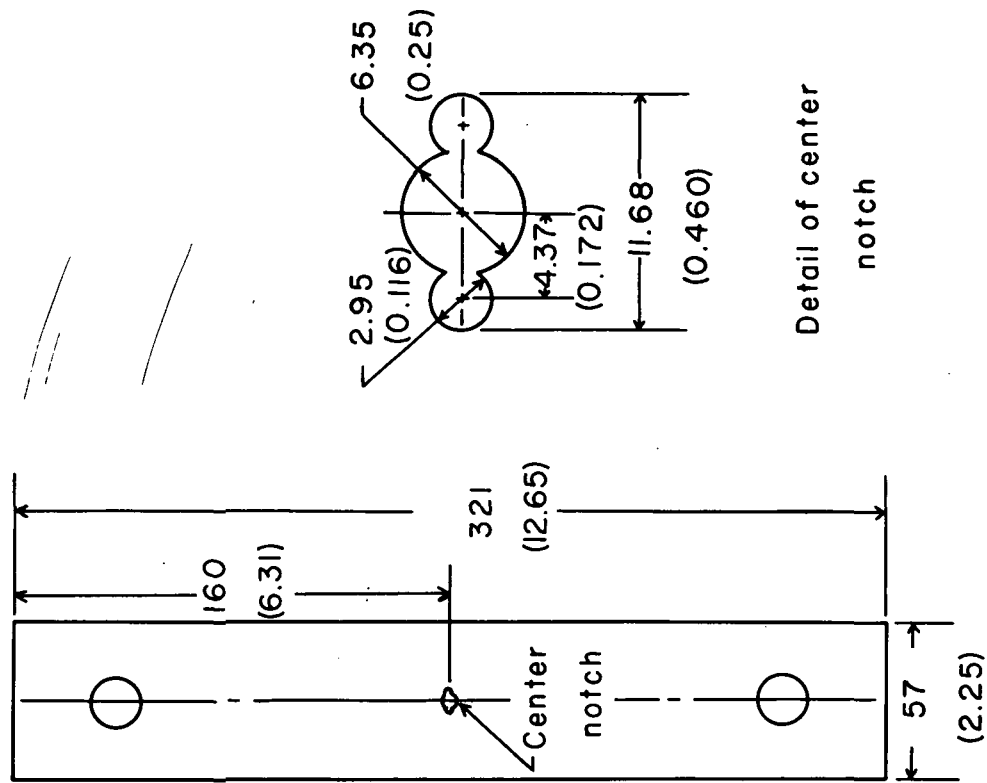TABLE IV.- RESULTS OF FATIGUE-CRACK-PROPAGATION EXPERIMENTS (R = 0.02)

Specimen number	S_{max} MN/m²	S_{max} psi	Number of cycles required to propagate a crack from a half-length a of 2.54 mm (0.10 in.) to a half-length of —								
			3.81 mm (0.15 in.)	5.08 mm (0.20 in.)	6.35 mm (0.25 in.)	7.62 mm (0.30 in.)	8.89 mm (0.35 in.)	10.16 mm (0.40 in.)	11.43 mm (0.45 in.)	12.70 mm (0.50 in.)	13.97 mm (0.55 in.)
(a) Air pressure, 101 kPa (760 torr)											
B58N7-10	276	40 000	520	730	870	960	1 000				
B52N7-8	276	40 000	690	930	1 070	1 160					
B52N7-10	207	30 000	1 100	1 850	2 300	2 500	2 650				
B51N7-10	207	30 000	1 400	2 000	2 350	2 650	2 850				
B59N7-10	138	20 000	3 500	5 800	7 500	8 600	9 300	9 900	10 300		
B57N7-2	138	20 000	3 500	5 900	7 500	8 700	9 500	10 100	10 400	10 700	
B57N7-4	103	15 000	7 500	12 500	16 000	18 500	20 500	22 000	23 000	24 000	24 500
B58N7-6	103	15 000	7 000	11 000	15 500	17 500	19 000	21 000	22 000	22 500	23 000
B56N7-2	69	10 000	35 500	51 500	60 000	67 000	72 000	76 000	79 000	81 500	83 500
B53N7-6	69	10 000	36 000	49 000	58 000	64 500	69 500	73 500	76 500	79 000	82 000
(b) Air pressure, 7 μPa (5 × 10⁻⁸ torr)											
B53N7-10	276	40 000	530	720	810	900					
B57N7-6	276	40 000	680	1 010	1 160	1 240	1 290				
B60N7-6	207	30 000	2 600	3 550	4 050	4 350	4 550				
B57N7-10	207	30 000	1 800	2 550	2 950	3 200	3 400				
B56N7-10	138	20 000	5 200	9 500	12 200	13 700	14 500	15 000	15 400		
B55N7-4	138	20 000	7 300	11 700	14 100	15 700	16 900	17 600	18 100		
B55N7-4	103	15 000	15 500	26 500	33 500	39 000	42 500	45 000	47 000	48 000	49 000
B56N7-6	103	15 000	20 000	31 000	37 500	42 500	45 500	48 000	49 500	50 500	51 500

TABLE V.- RESULTS OF FRACTURE-TOUGHNESS EXPERIMENTS

Specimen number	a_c		P_c		K_c	
	mm	in.	kN	lbf	$MN/m^{3/2}$	$psi-in^{1/2}$
(a) Air pressure, 101 kPa (760 torr)						
B59N7-10	12.7	0.50	29.3	6 580	56.9	51 800
B58N7-6	15.0	.59	24.6	5 540	55.0	50 000
B58N7-10	10.7	.42	37.2	8 370	61.6	56 100
B57N7-4	15.0	.59	24.5	5 500	53.7	48 900
B55N7-10	6.6	.26	44.4	9 980	54.6	49 700
B52N7-10	10.2	.40	36.0	8 090	58.7	53 400
B57N7-8	5.6	.22	49.4	11 100	54.2	49 300
B53N7-6	16.0	.63	22.2	4 980	45.7	41 600
B52N7-8	9.9	.39	36.0	8 090	57.5	52 300
B56N7-2	14.7	.58	23.0	5 170	50.5	46 000
B57N7-2	13.7	.54	28.7	6 450	57.9	52 600
B51N7-10	10.7	.42	33.2	7 460	56.6	51 500
(b) Air pressure, 7 μPa (5×10^{-8} torr)						
B56N7-6	16.3	0.64	23.4	5 260	57.6	52 400
B55N7-4	17.0	.67	18.9	4 250	49.1	44 700
B56N7-10	11.9	.47	29.5	6 640	53.3	48 500
B55N7-6	11.9	.47	28.6	6 420	52.5	47 800
B60N7-6	10.2	.40	33.3	7 490	54.3	49 400
B57N7-10	10.7	.42	34.7	7 810	57.0	51 900
B53N7-10	9.9	.39	38.3	8 600	61.6	56 100
B57N7-6	10.2	.40	33.9	7 610	54.0	49 100
B58N7-4	6.1	.24	46.1	10 370	55.8	50 800
B53N7-2	7.1	.28	44.9	10 090	58.1	52 900

6.35
(0.25)

2.95
(0.116)

4.37
(0.172)

11.68
(0.460)

Detail of center notch

321
(12.65)

160
(6.31)

Center notch

57
(2.25)

(b) Notched, $K_T = 4.1$.

321
(12.65)

160
(6.31)

19
(.75)

18(0.69) Diam.

51
(2)

191(7.5) Rad.

(a) Unnotched, $K_T = 1$.

Material thickness was 2.3 mm (0.090 in.). Dimensions are in mm (in.).
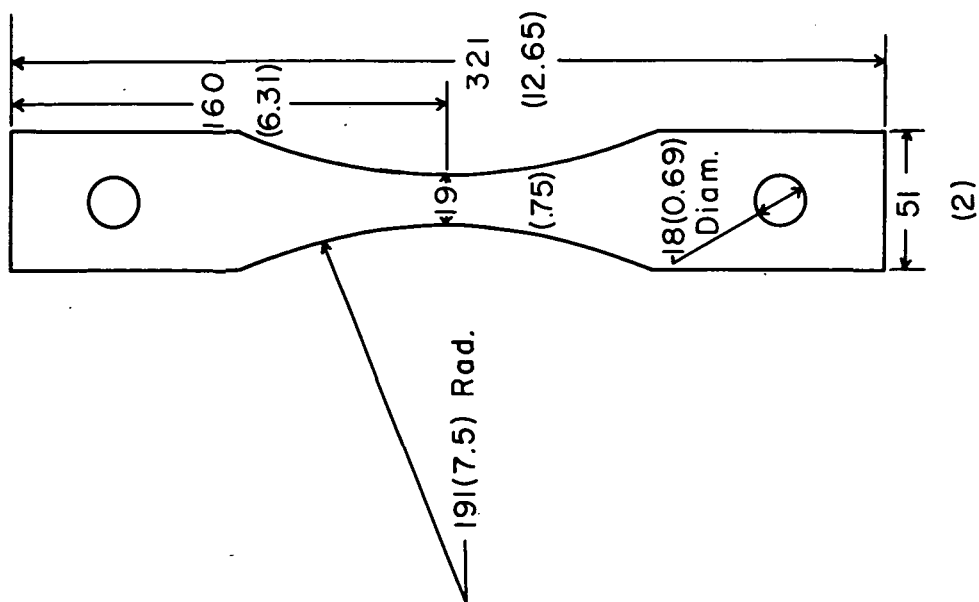
Figure 1.- Configurations of fatigue-life specimens.

Figure 2.- Configuration of the fatigue-crack-propagation and fracture
   toughness specimens.   Material thickness was 2.3 mm (0.090 in.).
   Dimensions are in mm (in.).
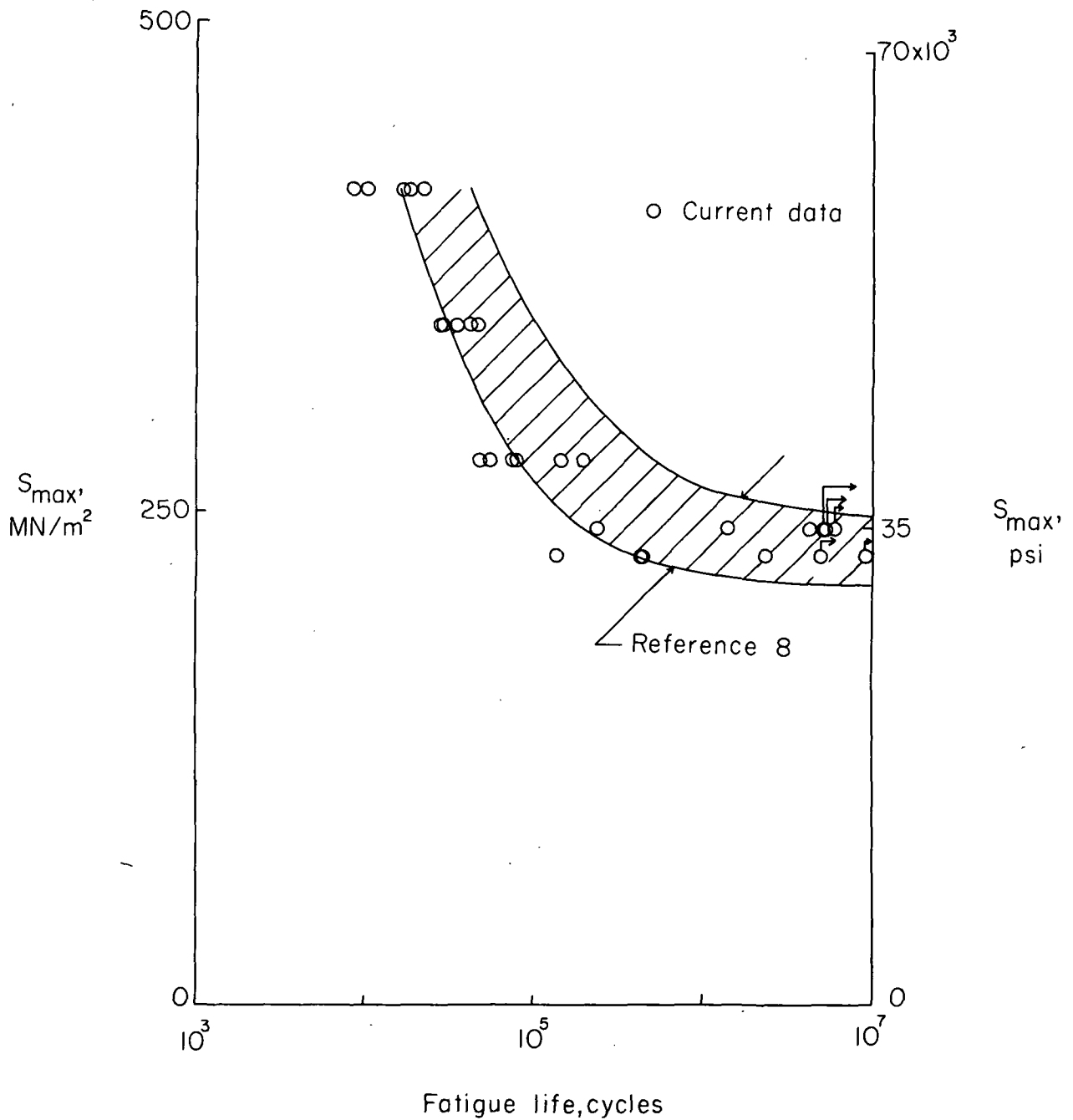
Figure 3.- Fatigue life of 7075-T6 aluminum alloy before and after 20 years' storage.
Air pressure, 101 kPa (760 torr); R = 0.02 for data points; R = 0 for scatter band.
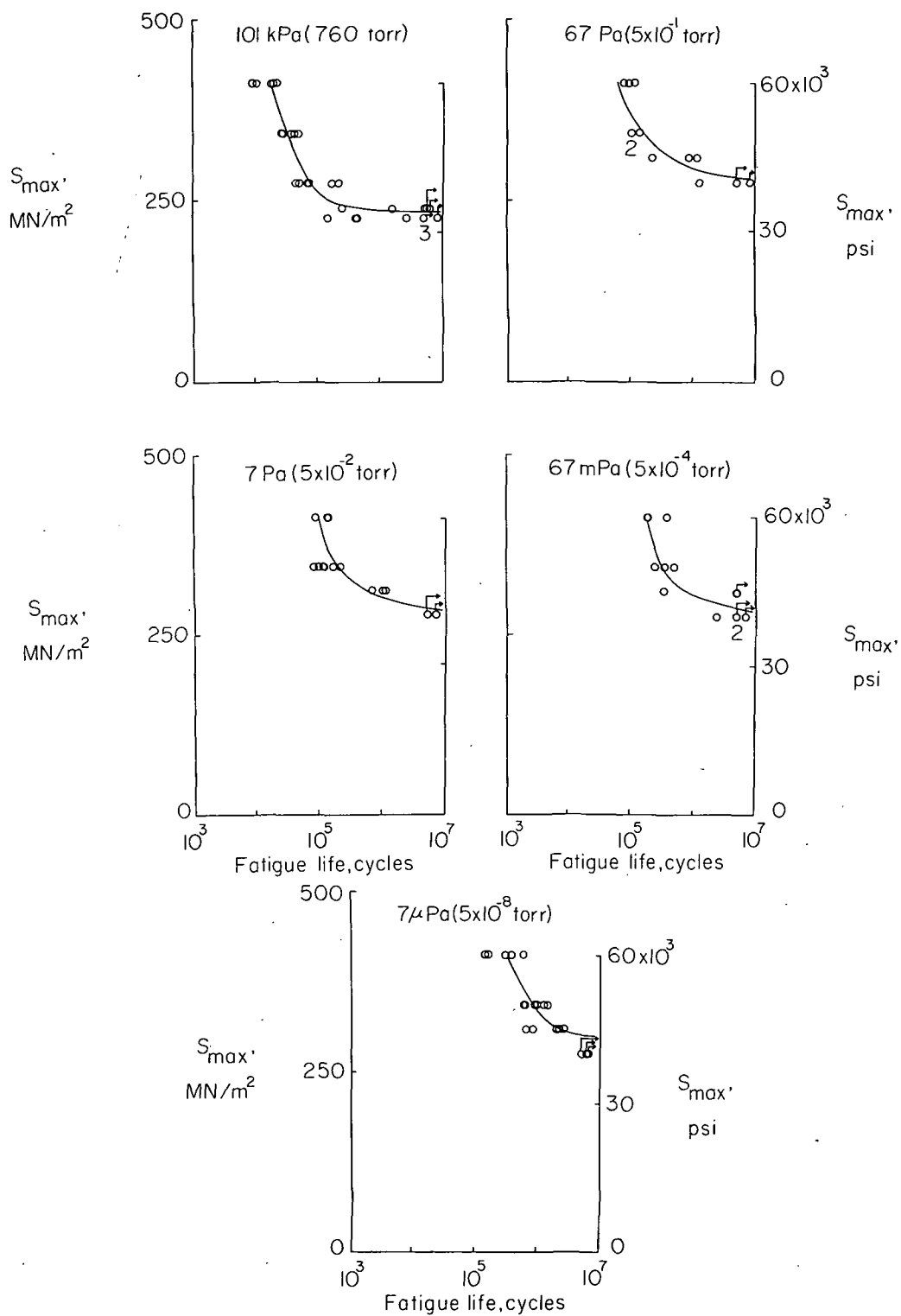
Figure 4.- Variation of the fatigue life of unnotched specimens of 7075-T6 aluminum alloy with stress and air pressure.   R = 0.02.
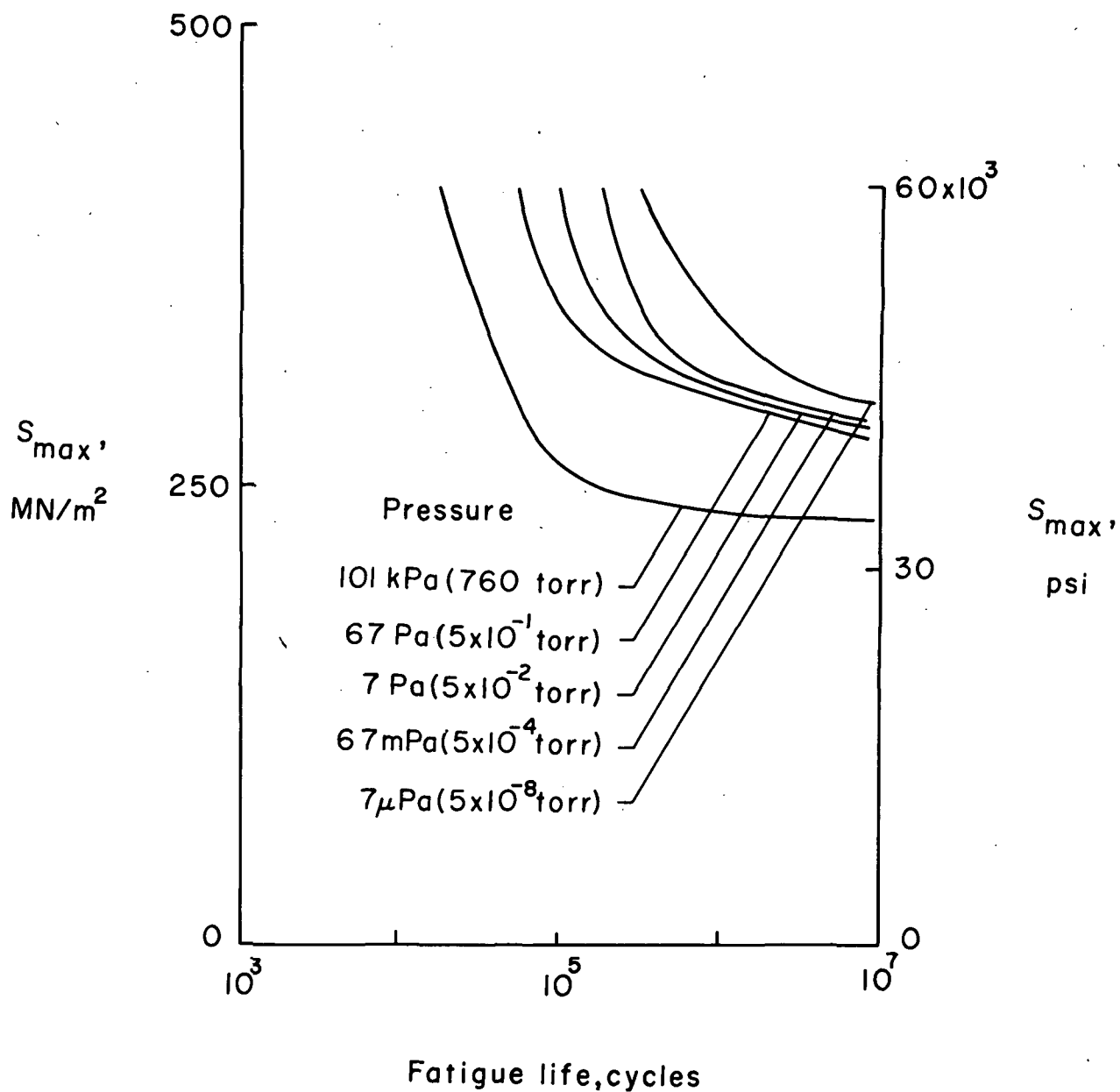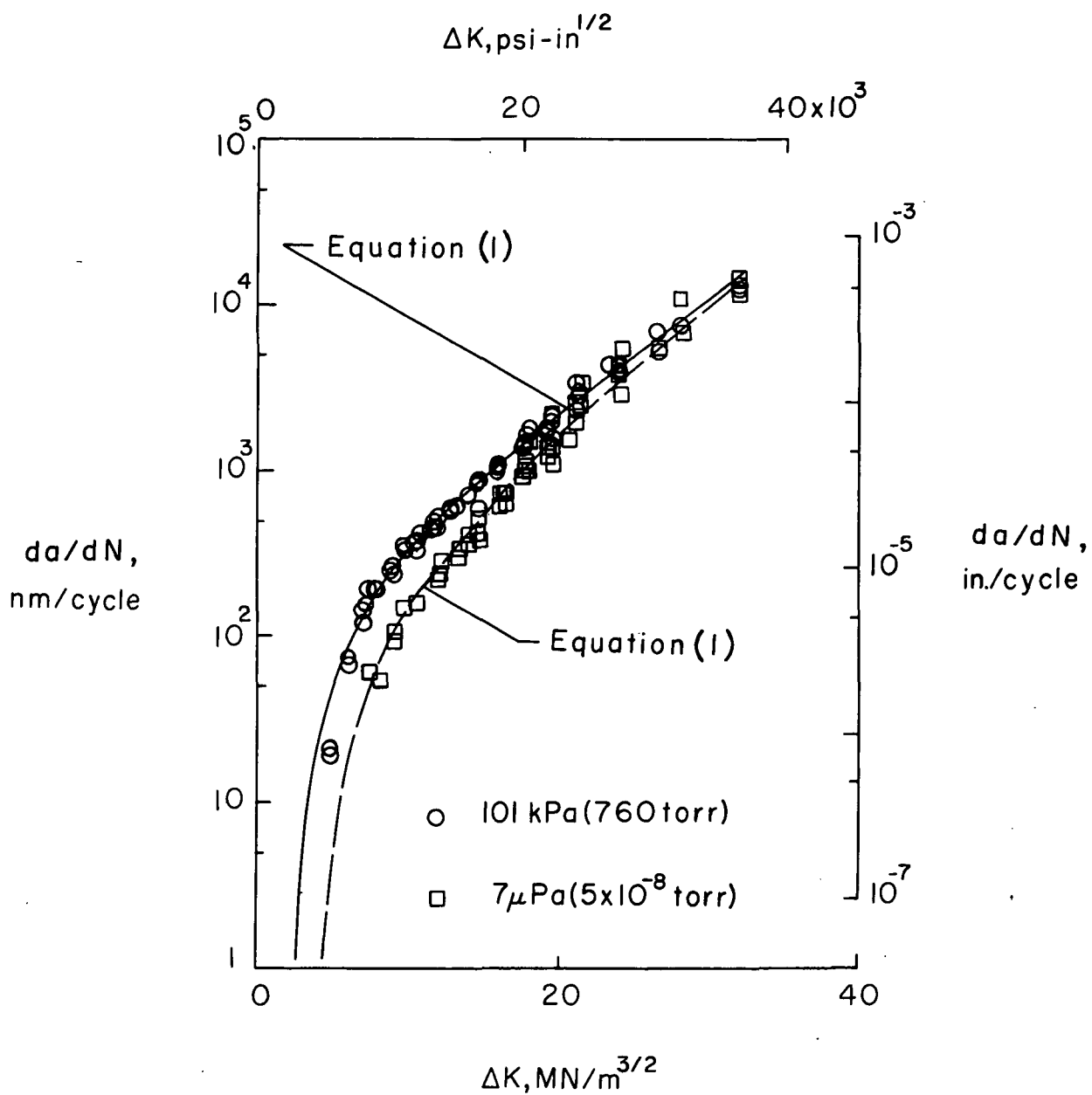
Figure 5.- Effect of air pressure on the fatigue life of unnotched
specimens of 7075-T6 aluminum alloy.   R = 0.02.
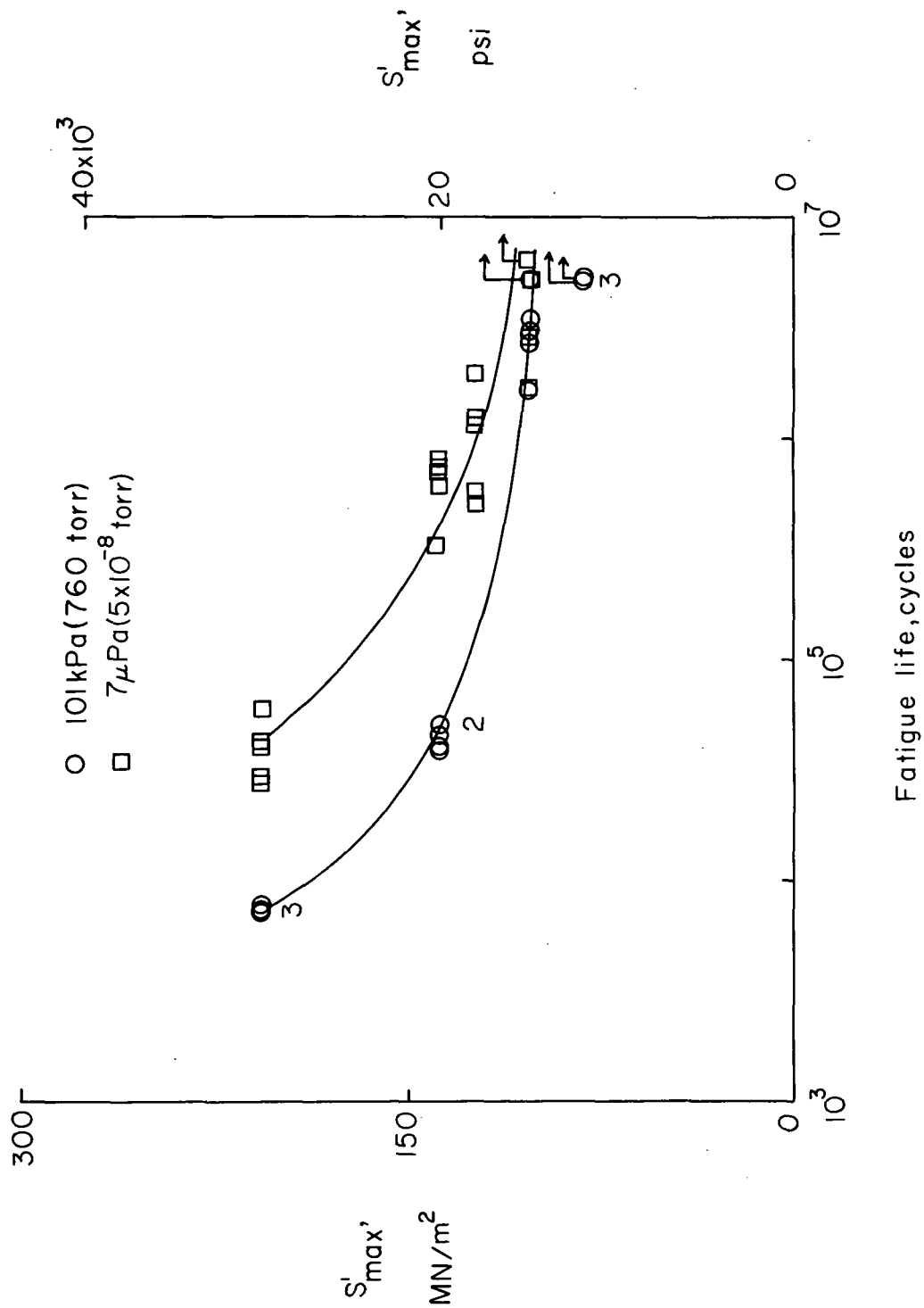
Figure 6.- Variation of fatigue life of notched specimens of 7075-T6 aluminum alloy with stress and air pressure. $K_T = 4.1$; $R = 0.02$.

30

Figure 7.- Variation of fatigue-crack-propagation rate with ΔK in vacuum and at atmospheric pressure. R = 0.02.
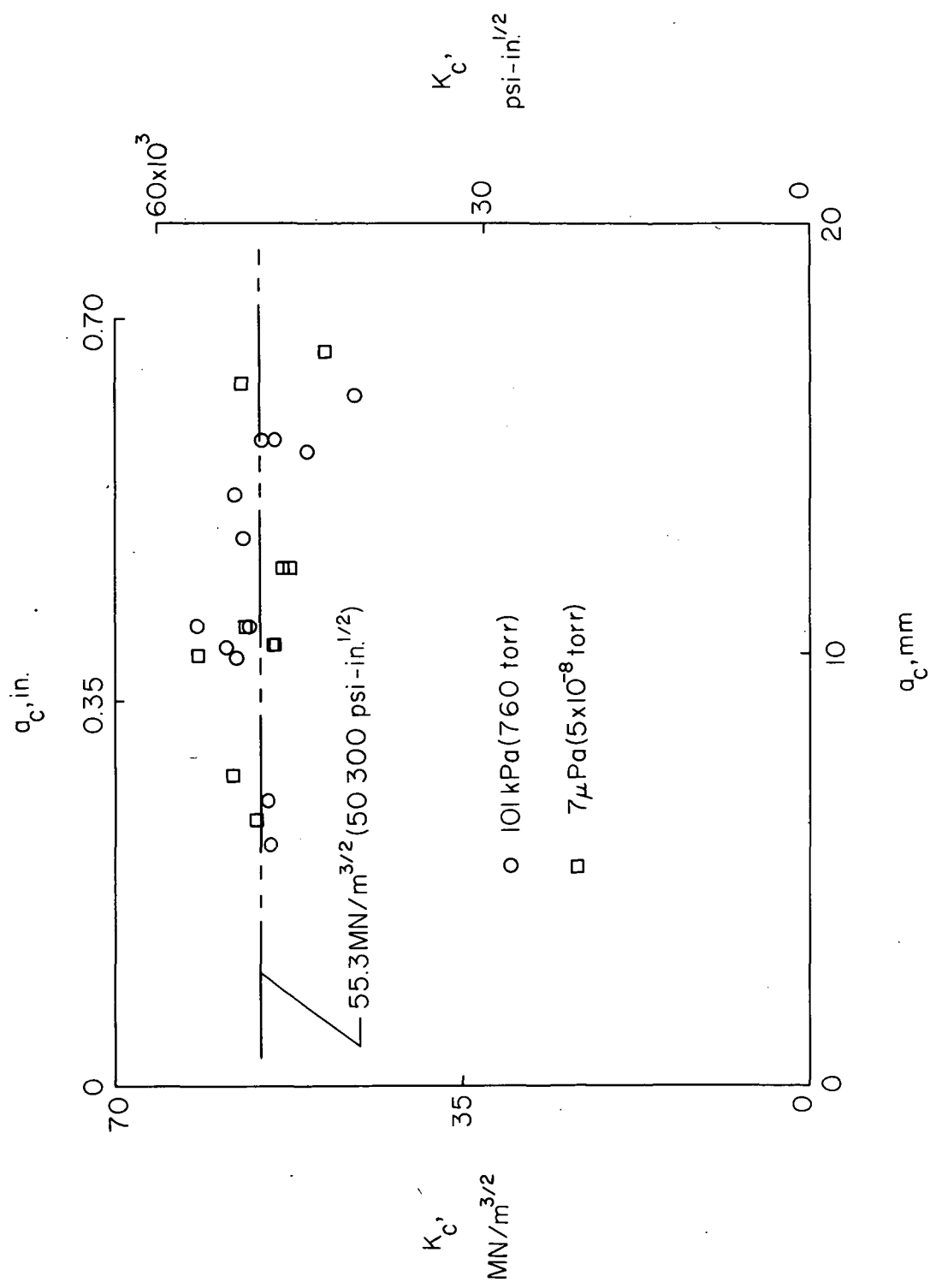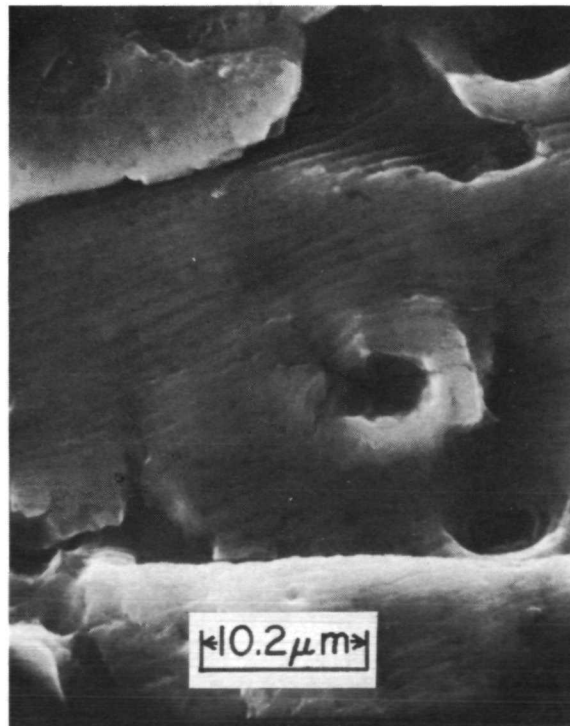
Figure 8.- Variation of K_c with a_c in vacuum and at atmospheric pressure.
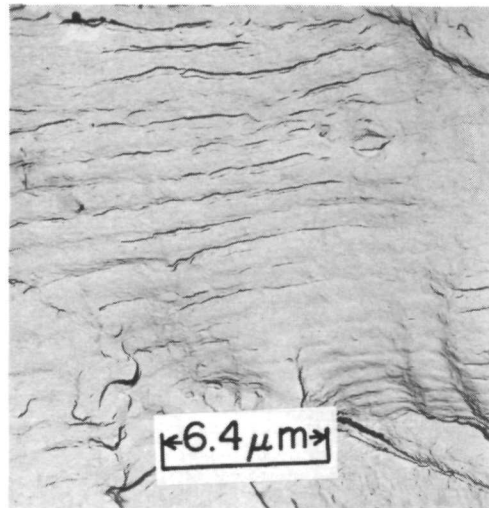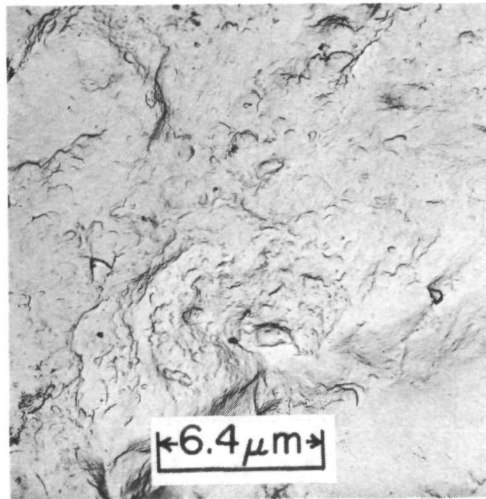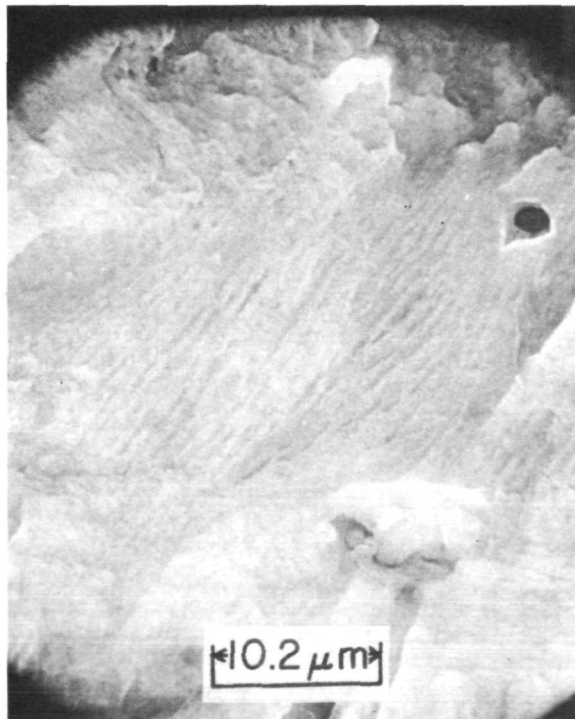
(a) Transmission electron microscope.

(b) Scanning electron microscope.   L-73-6811

Figure 9.- Fractographs of an unnotched specimen tested in air at
101 kPa (760 torr). S_{max} = 345 MN/m^2 (50 000 psi); R = 0.02.

(a) Transmission electron microscope.

(b) Scanning electron microscope.   L-73-6812

Figure 10.- Fractographs of an unnotched specimen tested in vacuum of
7 μPa (5 $\times$ 10^{-8} torr). S_{max} = 345 MN/m^2 (50 000 psi); R = 0.02.

A. Thermocouple gage
B. Ionization gage
C. Variable leak valve
D. Electrical power feed-throughs
E. Thermocouple feed-throughs
F. LN_2 supply and exhaust for lower cryopanel
G. LN_2 supply and exhaust for upper cryopanel
H. Specimen-viewing port
I. Flexible metal-bellows seal
J. Upper portion of vacuum chamber
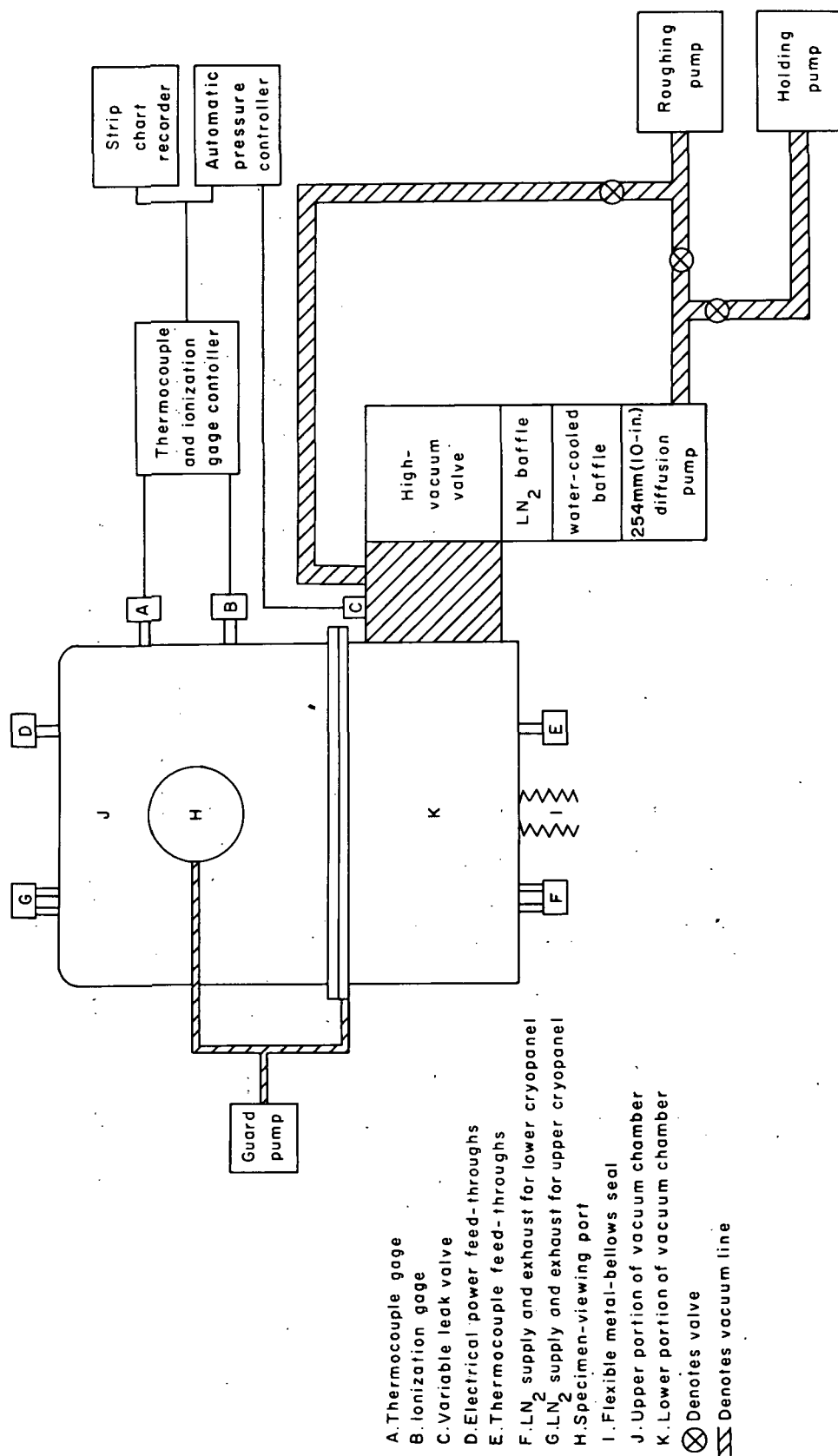K. Lower portion of vacuum chamber
⊗ Denotes valve
▨ Denotes vacuum line

Figure 11.- Schematic diagram of the vacuum-pumping system.
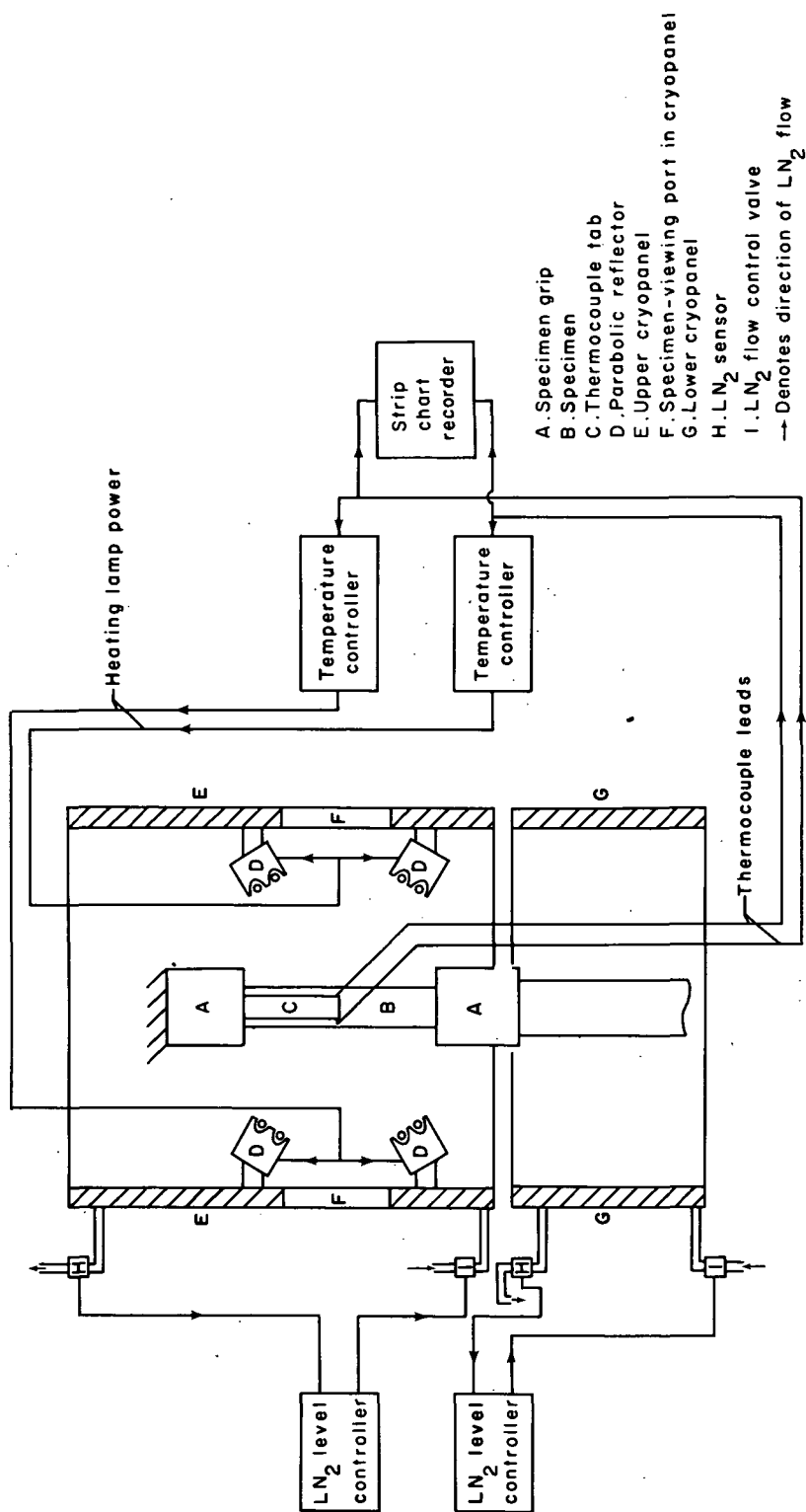
Figure 12.- Schematic diagram of the specimen temperature-control system.

A. Specimen grip
B. Specimen
C. Thermocouple tab
D. Parabolic reflector
E. Upper cryopanel
F. Specimen-viewing port in cryopanel
G. Lower cryopanel
H. LN$_2$ sensor
I. LN$_2$ flow control valve
→ Denotes direction of LN$_2$ flow

*"The aeronautical and space activities of the United States shall be
conducted so as to contribute . . . to the expansion of human knowl-
edge of phenomena in the atmosphere and space. The Administration
shall provide for the widest practicable and appropriate dissemination .
of information concerning its activities and the results thereof."*
—NATIONAL AERONAUTICS AND SPACE ACT OF 1958

NASA SCIENTIFIC AND TECHNICAL PUBLICATIONS

TECHNICAL REPORTS: Scientific and
technical information considered important,
complete, and a lasting contribution to existing
knowledge.

TECHNICAL NOTES: Information less broad
in scope but nevertheless of importance as a
contribution to existing knowledge.

TECHNICAL MEMORANDUMS:
Information receiving limited distribution
because of preliminary data, security classifica-
tion, or other reasons. Also includes conference
proceedings with either limited or unlimited
distribution.

CONTRACTOR REPORTS: Scientific and
technical information generated under a NASA
contract or grant and considered an important
contribution to existing knowledge.

TECHNICAL TRANSLATIONS: Information
published in a foreign language considered
to merit NASA distribution in English.

SPECIAL PUBLICATIONS: Information
derived from or of value to NASA activities.
Publications include final reports of major
projects, monographs, data compilations,
handbooks, sourcebooks, and special
bibliographies.

**TECHNOLOGY UTILIZATION
PUBLICATIONS**: Information on technology
used by NASA that may be of particular
interest in commercial and other non-aerospace
applications. Publications include Tech Briefs,
Technology Utilization Reports and
Technology Surveys.

Details on the availability of these publications may be obtained from:

SCIENTIFIC AND TECHNICAL INFORMATION OFFICE

NATIONAL AERONAUTICS AND SPACE ADMINISTRATION
Washington, D.C. 20546